Characterization of nano-structured magnesium-chromium ferrites synthesized by citrate-gel auto combustion method

M. Raghasudha[1], D. Ravinder[2*], P. Veerasomaiah[3]

[1]Department of Chemistry, Jayaprakash Narayan College of Engineering, Mahabubnagar 509001, Andhra Pradesh, India
[2]Department of Physics, Nizam College, Basheerbagh Osmania University, Hyderabad 500001, Andhra Pradesh, India
[3]Department of Chemistry, Osmania University, Hyderabad 500007, Andhra Pradesh, India

*Corresponding author. Tel: (+91) 9246162228; E-mail: ravindergupta28@rediffmail.com; raghasudha_m@yahoo.co.in

ABSTRACT

Nano-ferrites of the composition Mg Cr_x $Fe_{2-x}O_4$ (where x=0.0, 0.1, 0.3, 0.5, 0.7, 0.9 and 1.0) were synthesized at a very low temperature (180°C) by Citrate-gel auto combustion method. The as synthesized powders were sintered at 500^0C for four hours in an air and were characterized by X-ray diffraction (XRD) which confirmed the formation of cubic spinel structure of ferrites. The crystallite size was in the range of 7 to 23nm for different compositions with the significant decrease of ~16nm in response to the increase in Cr substitution. Such low nano sized ferrites are desirable for variety of applications like, in magnetic data storage and in targeted drug delivery, etc. Morphological studies by Scanning Electron Microscopy (SEM) revealed formation of largely agglomerated, well defined nano particles of the sample. Elemental composition characterizations of the prepared samples were performed by Energy Dispersive Spectroscopy (EDS) which shows the presence of Mg, Cr, Fe and O without precipitating cations. The FTIR spectral studies at room temperature in the range of 400 to 800cm^{-1} showed two strong absorption bands. The high frequency band (v_1) around 600 cm^{-1} is attributed to the intrinsic vibrations of tetrahedral complexes and the low frequency band (v_2) around 400 cm^{-1} is due to octahedral complexes. The spectra showed the characteristic peaks of ferrite sample. The observed results can be explained on the basis of composition and crystal size. Copyright © 2013 VBRI press.

Keywords: Nano-ferrites; citrate-gel auto combustion; X-ray diffraction; SEM; EDS; FTIR.

M. Raghasudha is working as Associate Professor in Chemistry, Jayaprakash Narayan college of Engineering, Mahabubnagar, Andhra Pradesh, India. She obtained her M.Sc. in Chemistry (1997) from Kakatiya University, Andhra Pradesh and M.Phil. in Chemistry (2007) from Alagappa University, Tamil Nadu. She has submitted her Ph.D. thesis to Osmania University in August 2013. She has published 5 research papers in International Journals and has 16 years of teaching experience. Her current area of research is on electrical and magnetic properties of ferrite nano materials and thin films by citrate-gel method.

D. Ravinder is working as Professor and Head, Department of Physics, Nizam college, Osmania University, Hyderabad, Andhra Pradesh, India. His research work is on magnetic and electrical properties of ferrites, thin films, GMR materials, Cu-Co alloy thin films and nano-materials by pulsed laser deposition, sol gel, citrate precursor method and electro deposition. To his credit, he has published 150 research papers in International Journals. He has been awarded Young Scientist award received by Dr. Abdual Kalam (former president of India), for outstanding contributions in the field of science and

Technology, UGC research award, Boyscast by DST (Department of science and technology), Government of India, JSPS fellowship Japan and Royal Society fellowship, UK . He also visited USA, UK, Sweden, Ireland, Singapore and Japan for Collaborative Research and invited talks.

P. Veera Somaiah is currently working as Professor in the Department of Chemistry, Osmania University, Hyderabad. He did his M.Sc. and Ph.D. in Chemistry from Osmania University and pursued his Post Doctoral Research in Chemical kinetics field at University of Durban, South Africa. His areas of interest include chemical kinetics, Spectroscopy, Material science and Polymers.

Introduction

Research on nanoparticles has opened an avenue for various potential applications due to their novel properties. More specifically materials with nano scale dimensions 1-100 nm show extraordinary physical and chemical properties. The reduction in the size of the nanoparticles

leads to increase in relative surface area. The quantum size effect and the large surface area of nanoparticles dramatically change some of the magnetic properties and exhibit super paramagnetic phenomena and quantum tunneling of magnetization, because each particle behaves as single magnetic domain [1]. Nanomaterials therefore play a very prominent role in physical, chemical and biomedical applications due to their high surface energies. Among such materials Ferrites are useful magnetic materials because of their versatility, low cost and high electromagnetic performance over a wide frequency range [2]. Spinel type ferrites are commonly used in many electronic and magnetic devices due to their high magnetic permeability and low magnetic losses [3]. Usually ferrite materials have low conductivity i.e. high resistivity which greatly influences the dielectric and magnetic behavior of ferrites [4]. Due to their high thermodynamic stability, low electrical conductivity, electro catalytic activity and resistance to corrosion these materials are used for high temperature applications [5]. The magnetic properties of the nanosized ferrites are entirely different from those of their bulk counterparts, such as the super paramagnetic behavior and associated properties. Nanosized ferrites with uniform particle size and narrow size distribution are desirable for a variety of applications like targeted drug delivery, medical imaging, magnetic data storage and other biomedical applications, etc. [6].

Magnesium ferrite belongs to a class of compounds having the general formula $M^{+2}Fe^{+3}_2O_4$ (and also AB_2O_4) crystallizing with spinel structure (where M represents tetrahedral site and Fe represents the octahedral site)[7]. The interesting properties of spinel ferrites arise from their ability to distribute the cations among the tetrahedral (A) and Octahedral (B) sites [8]. For obtaining the specific properties ferrites can be fabricated by substituting various magnetic and non-magnetic ions which greatly affect the magnetic moments, lattice parameters and exchange interactions [9, 10]. Magnesium nano ferrites are the potential materials for various applications due to their high electrical resistivity, low magnetic and dielectric losses [11,12]. Doping of $MgFe_2O_4$ with one or several metals is the best method to alter its properties. Several researchers have reported the synthesis of Mg-Cr ferrites using different techniques such as Double Sintering technique [13], Solid state ceramic sintering technique [14], Micro emulsion method [15], Coprecipitation technique [16]. To my knowledge a little information is available about the nano sized Mg-Cr ferrites formed by Citrate-Gel Auto combustion method. The Citrate-Gel method is a simple process which speeds up the synthesis of complex materials. This method offers significant saving in time, energy consumption over the traditional methods. In this method the metal ions or complexes are immobilized on atomic scale which allows obtaining oxides at temperature lower than that produced in solid state reaction. This method also produces homogeneous and stoichiometric oxides [17].

In this work we prepared Nano-ferrites of the composition $MgCr_xFe_{2-x}O_4$ (where x=0.0, 0.1, 0.3, 0.5, 0.7, 0.9 and 1.0) by Citrate-Gel method with a very low particles size with the assumption that the magnetic, electrical and dielectric properties would be improved by substitution of Fe^{+3} with Cr^{+3} ions. As per the authors knowledge it is the first observation of Mg-Cr nano ferrites obtained with low particles size by citrate-gel method. In this paper, we present the Synthesis, XRD, SEM, EDS and FTIR studies of Chromium doped Magnesium ferrites using the Citrate gel method.

Experimental

Materials

Mg-Cr Nano ferrites having the chemical formula $MgCr_xFe_{2-x}O_4$ (where x=0.0, 0.1, 0.3, 0.5, 0.7, 0.9 and 1.0) were synthesized by Citrate-Gel auto combustion technique using magnesium nitrate ($Mg(NO_3)_26H_2O$, 99%, SD Fine Chem. Ltd. Mumbai, India), ferric nitrate ($Fe(NO_3)_29H_2O$, GR grade, Otto Chemie Pvt. Ltd. Mumbai, India), chromium nitrate ($Cr(NO_3)_29H_2O$, GR grade, Otto Chemie Pvt. Ltd. Mumbai, India), citric acid ($C_6H_8O_7.H_2O$, AR grade, SD Fine Chem. Ltd. Mumbai, India) and ammonia (NH_3, AR grade, SD Fine Chem. Ltd. Mumbai, India).

Chemical reaction

$Mg(NO_3)_26H_2O + 2\ Fe(NO_3)_29H_2O + C_6H_8O_7.H_2O \rightarrow$
$MgFe_2O_4 + 29H_2O + 4N_2 + 6CO_2 + 5.5O_2$
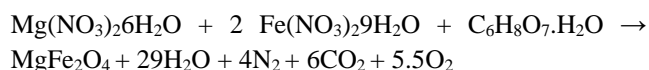
Synthesis

Calculated quantities of above nitrate salts were dissolved in double distilled water and required amount of aqueous citric acid solution was added as chelating agent. The mixture was thoroughly stirred to get a homogeneous solution. Ammonia solution was added to this nitrate-citrate mixture to adjust the p^H to 7. The mixed solution was heated at about 100^0C with uniform stirring and evaporated to obtain a highly viscous gel denoted as precursor. The resultant gel was further heated on a hot plate maintained at a temperature of 180^0C to 200^0C. When finally all water molecules were removed from the mixture, the viscous gel began frothing. The gel gave a fast flameless auto combustion reaction with the evolution of large amounts of gaseous products (shown in the above chemical reaction). It started in the hottest zones of the beaker and propagated from the bottom to the top like the eruption of a Volcano. The reaction was completed in a minute giving rise to dark grey voluminous product with a structure similar to Branched tree. Finally the burnt powder was ground and was calcined in air at temperature 500^0C for four hours to obtain a spinal phase. The synthesis is shown in **Fig. 1** in the form of Flow chart.

Characterization

The structural characterization of the synthesized samples was carried out by Phillips X ray diffractometer (model 3710) using Cu Kα radiation (λ=1.5405A^0) at room temperature by continuous scanning in the range of $2\theta^0$ to $85\ \theta^0$ to investigate the phase and crystallite size. The Morphology of the samples was studied by Scanning Electron Microscope (SEM). Elemental analysis was carried out by using Energy Dispersive Spectrometer (EDS). The infrared spectra of synthesized Mg-Cr nano-ferrite powders (as pellets in KBr) were recorded by

SHIMADZU Fourier Transform Infrared Spectrophotometer (model P/N-206-73500-38) in the range of 400 to 800 cm^{-1} with a resolution of 1cm^{-1} which confirms the formation of a single phase cubic spinel.
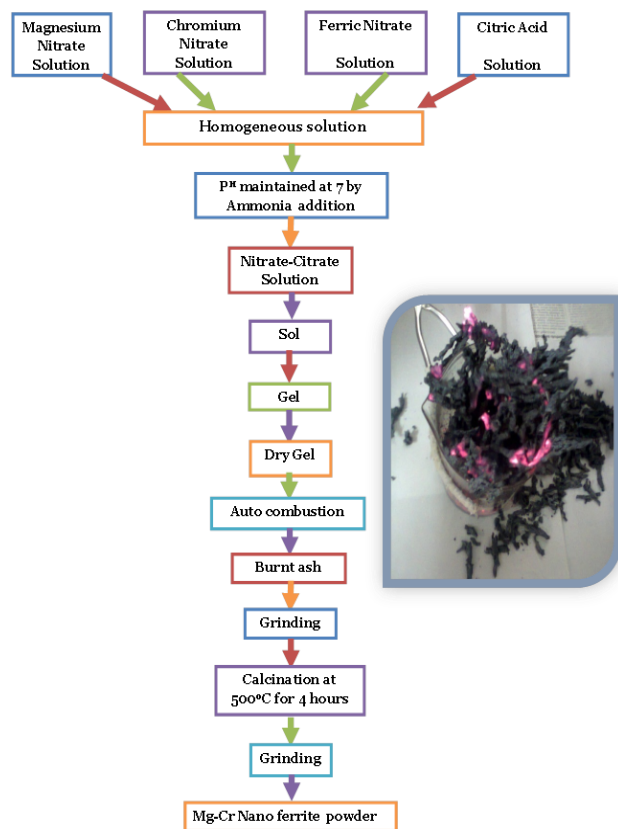

Fig. 1. Flow Chart for the synthesis of Mg-Cr Nano ferrites.

Results and discussions
XRD analysis

The structural characterization of all the nano-ferrites was carried out by X-ray Diffraction. From the analysis the 2theta and intensity data was used and graphs were plotted as shown in **Fig. 2**. The X-ray diffraction pattern, crystalline phases were identified by comparison with reference data from the ICSD card No. 71-1232 for Magnesium ferrites. All Bragg reflections have been indexed which confirms the formation of a well-defined single phase cubic spinel structure without any impurity peak. The strongest reflection comes from (311) plane that indicates spinel phase. Fundamental reflections from the crystal planes (111), (220), (311), (400), (511) and (440), characterizing the spinel ferrites are clearly identified. Reflections from the planes (111), (220) and (511) have been observed with weak intensities. The XRD patterns of all the Chromium substituted Magnesium ferrites showed the homogeneous single phased cubic spinel belonging to the space group Fd3m (confirmed by ICSD Ref 71-1232).

The crystallite size (D) was calculated for all the compositions using maximum intensity peak (311) from Scherrer's formula **[18]**.

$$Crystallite\,size = D = 0.91\lambda/\beta\cos\theta$$

where, λ = wavelength of X-ray, β = Full width half maximum (radians), θ = Bragg's angle at the peak position.

The crystallite size was in the range of 7 to 23nm (shown in the **Table 1**) for different compositions with the significant decrease of ~16nm in response to the increase in Cr substitution. To my knowledge no other method has resulted the Mg-Cr ferrites with such a small size except the citrate – Gel Auto combustion method. Conventional methods need a very high temperature and prolonged heating time **[13, 14]**.

Advantages of Citrate gel method over the conventional methods are (1) simple and economic method (2) use of relatively simple equipment (3) formation of high purity products (4) good stoichiometric control (5) production of ultra-fine particles with a narrow size distribution (6) short processing time (7) very low processing temperature (8) low sintering temperature.

Lattice parameter (a) of the individual composition was calculated by using the following formula and were tabulated in **Table 1.**

$$a = d\sqrt{h^2 + k^2 + l^2}$$

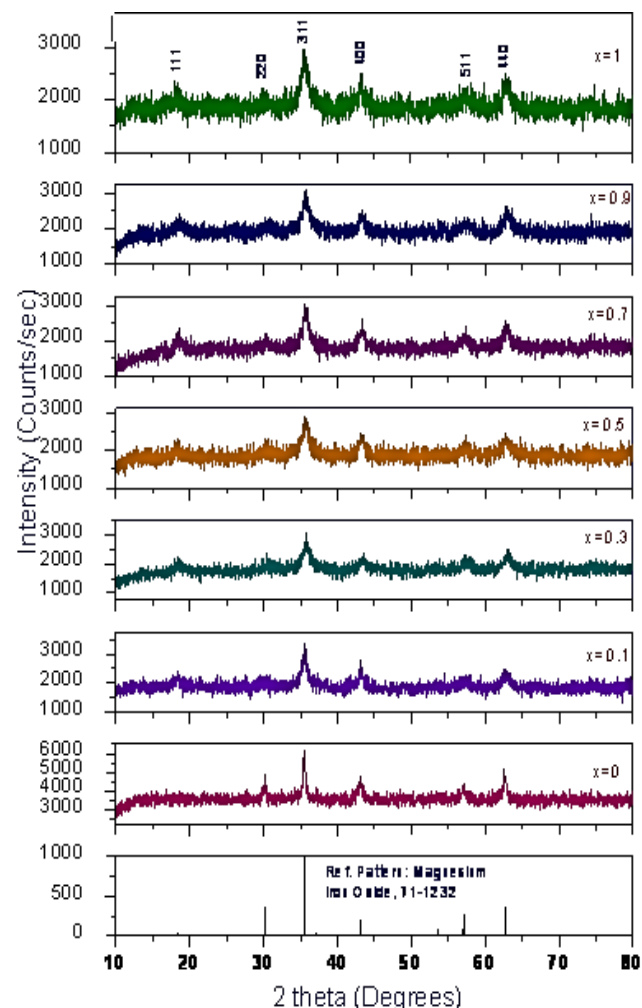where, a = lattice parameter, d = interplanar spacing and hkl = the miller indices.

Fig. 2. XRD of Mg Cr$_x$Fe$_{2-x}$O$_4$ (x = 0, 0.1, 0.3, 0.5, 0.7, 0.9, 1).

Table 1. Values Crystallite size (D_x) and lattice parameter (a) of Mg-Cr Ferrites.

Ferrite Composition	Crystallite size (nm)	Lattice parameter a (A^0)
$MgFe_2O_4$	23.469	8.382
$MgCr_{0.1}Fe_{1.9}o_4$	8.8989	8.378
$MgCr_{0.3}Fe_{1.7}o_4$	9.1137	8.368
$MgCr_{0.5}Fe_{1.5}o_4$	7.1662	8.357
$MgCr_{0.7}Fe_{1.3}o_4$	8.1328	8.346
$MgCr_{0.9}Fe_{1.1}o_4$	7.6449	8.338
$MgCrFeO_4$	7.6259	8.335
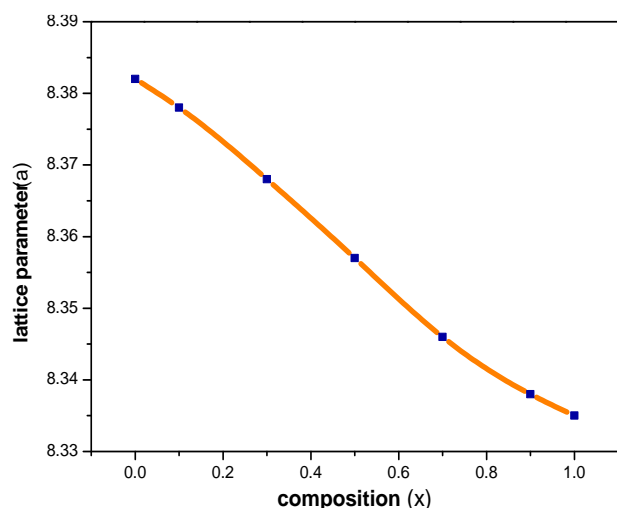
Fig. 3. Variation of lattice Parameter with Cr^{3+}content.

Table 2. Values of X-ray density (d_x) and volume of unit cell (V) of Mg-Cr Ferrites.

Ferrite Composition	x-ray density d_x (gm/cc)	Vol. of unit cell V
$MgFe_2O_4$	4.514	588.902
$MgCr_{0.1}Fe_{1.9}o_4$	4.505	588.059
$MgCr_{0.3}Fe_{1.7}o_4$	4.504	585.956
$MgCr_{0.5}Fe_{1.5}o_4$	4.503	583.648
$MgCr_{0.7}Fe_{1.3}o_4$	4.501	581.347
$MgCr_{0.9}Fe_{1.1}o_4$	4.499	579.676
$MgCrFeO_4$	4.499	579.051

A plot of the lattice parameter Vs Cr^{+3} compositions is shown in **Fig. 3**, which indicates the variation of lattice parameter with composition. The lattice parameter is found to decrease linearly with increase of Cr^{+3} ions in the Mg-Cr nano-ferrites system indicating that the system obeys Vegard's law [19]. The decrease in lattice parameter with increase in Cr^{+3} content is explained on the basis of the relative ionic radii of Cr^{+3} and Fe^{+3} ions. Since Cr^{+3} ions

have smaller ionic radii ($0.63A^0$) than those of Fe^{+3} ions ($0.64A^0$) in octahedral sites, a partial replacement of the Fe^{+3} ions by the Cr^{+3} ions causes shrinkage of unit cell dimensions resulting in decrease in the lattice parameter. The x-ray density (d_x) is calculated using the following formula [20] and were tabulated in **Table 2.**

$$x-ray density = d_x = 8M\big/Na^3\,(gm/cc)$$

where M=Molecular weight of the sample, N = Avagadro number, and a= lattice parameter.

A plot of the x-ray density (d_x) Vs Cr^{+3} compositions is shown in **Fig. 4** that indicates the variation of x-ray density (d_x) with composition. The X-ray density depends on the lattice parameter and molecular weight of the sample. In the present Mg-Cr system, with increase in the Cr^{+3} content it is observed that the molecular weight is decreased and the lattice parameter has also decreased. This may be due to greater atomic weight of Fe - 55.847 gm/mole and less atomic weight of Cr - 51.996 gm/mole. From the plot it is observed that x-ray density decreases with increase in Cr content (x), this is because the decrease in mass overtakes the decrease in volume of the unit cell. Hence X-ray density is decreased with increase in Cr^{+3} content.

Similar behavior of lattice parameter and X-ray density with Cr^{+3} composition was observed for the Mg-Cr ferrite system synthesized in the solid-state reaction method using conventional ceramic technique reported by Faizuna Nesa, A.K.M. Zakaria, M. A. Saeed khan, S.M. Yunus, A.K. Das. S.G. Eriksson **[14]**. Volume of the unit cell is calculated as;

$$V = a^3$$

in $(A^0)^3$ where 'a' is the lattice parameter.

The calculated values are tabulated in **Table 2**. It is observed that volume of the unit cell decreases with increase in Cr^{+3} content. It is because Volume of the unit cell depends on the lattice parameter which decreases with increase in Cr^{+3}content. The X-ray density (d_x) and volume of the unit cell (V) of Magnesium Ferrite were in good agreement with the reported values 4.518gm/cc and 588.06 $(A^0)^3$ from ICSD data.
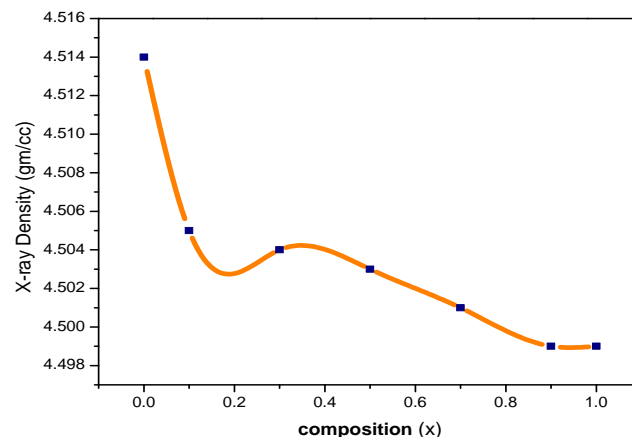
Fig. 4. Variation of x-ray density of Mg-Cr ferrites with Cr^{+3} content.

The distance between magnetic ions (hopping length) in A site (Tetrahedral) and B site (Octahedral) were calculated by using the following relations [21].

$$d_A = 0.25a\sqrt{3} \quad \text{and} \quad d_B = 0.25a\sqrt{2}$$

where 'a' is lattice parameter.

The values of the Hopping length for tetrahedral site (d_A) and octahedral site (d_B) were tabulated in **Table 3**.

Table 3. Values of hopping length for tetrahedral site (d_A) and octahedral site (d_B) of Mg-Cr Ferrites.

Ferrite Composition	A site d_A	B-site d_B
$MgFe_2O_4$	3.6295	2.9635
$MgCr_{0.1}Fe_{1.9}o_4$	3.6278	2.9620
$MgCr_{0.3}Fe_{1.7}o_4$	3.6234	2.9585
$MgCr_{0.5}Fe_{1.5}o_4$	3.6187	2.9546
$MgCr_{0.7}Fe_{1.3}o_4$	3.6139	2.9507
$MgCr_{0.9}Fe_{1.1}o_4$	3.6105	2.9479
$MgCrFeO_4$	3.6092	2.9468

The relation between hopping length for Octahedral and Tetrahedral sites as a function of Cr^{+3} content(x) was shown in **Fig. 5**. It is observed that the distance between the magnetic ions decreases as the Cr content increases. It may be explained due to the fact that Cr^{+3} ion has smaller radius ($0.63A^0$) than Fe^{+3} ion i.e. ($0.64A^0$) which makes the magnetic ions become closer to each other and hopping length decreases.

Similar behavior of hopping length with Cr^{+3} composition was observed for the Mg-Cr system synthesized by double sintering technique reported by V.B. Kawade, G.K. Bichile, K.M. Jadhav [13].

Morphology by SEM

The morphological analysis was performed using SEM (Scanning Electron Microscope). The secondary electron images were taken at different magnifications to study the morphology by SEM. **Fig. 6** shows SEM representative micrographs of the samples with different amounts of substitution.

It can be seen from SEM micrographs of various compositions that the morphology of the particles is similar. They reveal largely agglomerated, well defined nano particles of the sample powder with inhomogeneous broader grain size distribution. Such broader size distribution is characteristic of mechanically activated nano sized particles. The agglomeration of particles is also because they experience a permanent magnetic moment proportional to their volume [22].
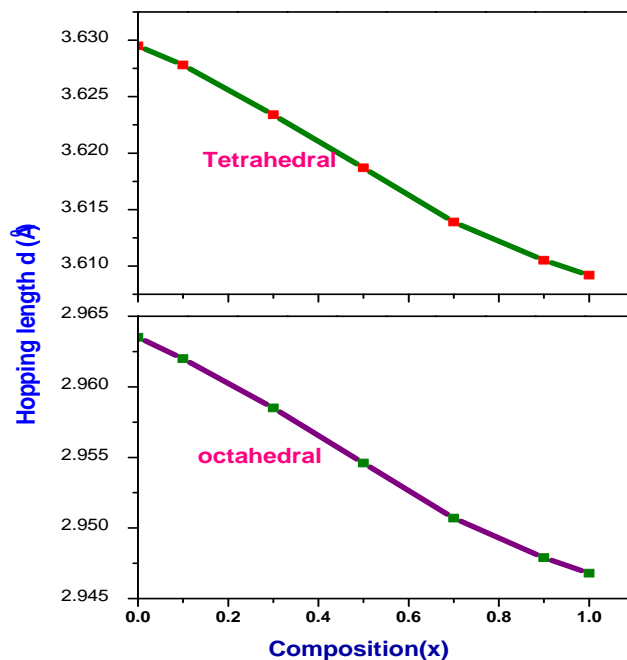

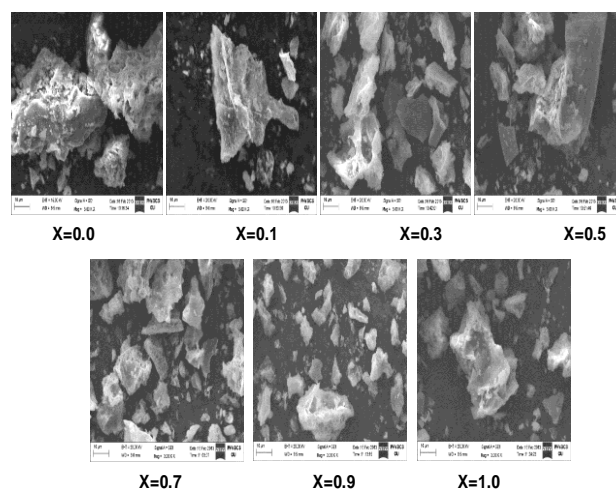**Fig. 5.** The distance between magnetic ions in both octahedral and tetrahedral sites as a function of *x*.

Fig. 6. SEM images of $MgCr_xFe_{2-x}O_4$ nano –ferrites.

Table 4. Elements of each sample composition Mg-Cr ferrites analyzed by (%weight) obtained by EDS.

Element	O		Mg		Cr		Fe	
Ferrite composition	Element %	Atomic %	Element %	Atomic %	Element %	Atomic %	Element %	Atomic %
$MgFe_2O_4$	18.49	40.74	9.54	13.83	-	-	71.97	45.43
$MgCr_{0.1}Fe_{1.9}O_4$	40.93	65.05	12.37	12.94	22.31	10.91	24.39	11.11
$MgCr_{0.3}Fe_{1.7}O_4$	40.1	64.38	12.22	12.91	22.98	11.35	24.7	11.36
$MgCr_{0.5}Fe_{1.5}O_4$	34.43	59.39	11.29	12.81	26.83	14.24	27.45	13.56
$MgCr_{0.7}Fe_{1.3}O_4$	36.30	61.11	11.62	12.88	25.21	13.06	26.87	12.96
$MgCr_{0.9}Fe_{1.1}O_4$	30.07	55.16	10.21	12.33	28.98	16.36	30.73	16.15
$MgCrFeO_4$	35.34	60.40	11.01	12.39	26.37	13.83	27.34	13.39

Heating results in the well-faceted grains to form solid bodies. It is a porous network of sintered bodies exhibiting foam like structure. An enlarged mass of compound formation was observed due to the influence of magnesium ions. The SEM micrographs also indicate that the particle size of the sample lies in the nanometer region. They

indicate that with increase in Cr composition the grain size is decreased (from x=0 to x=1).

Elemental analysis by EDS

The elemental analysis of all the Mg-Cr nano ferrite samples with different composition was analyzed by an Energy Dispersive Spectrometer (EDS) (**Fig. 7**) and the elemental % and atomic % of various elements in the samples were shown in **Table 4.**
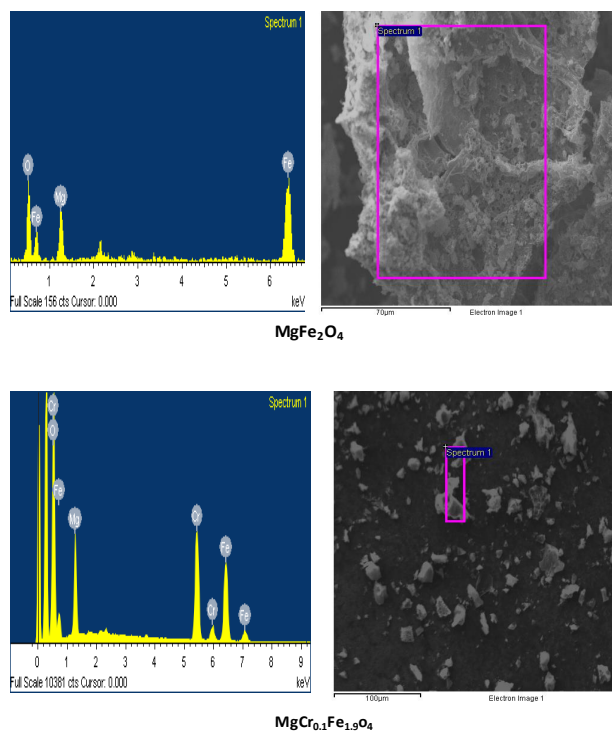

$MgFe_2O_4$

$MgCr_{0.1}Fe_{1.9}O_4$

Fig. 7. EDS graph of $MgCr_xFe_{2-x}O_4$ nano- ferrites with x=0.0, 0.1.

FTIR spectral analysis

The FTIR spectra of the $MgCr_xFe_{2-x}O4$ (x=0.0, 0.1, 0.3, 0.5, 0.7, 0.9, 1.0) system were recorded in the range of 200-800cm^{-1} which are shown in the **Fig. 8**. The spectra of all the ferrites have been used to locate the band positions which are given in the **Table 5**. In the present study the absorption bands ν_1 and ν_2 are found to be around 600cm^{-1} and 400cm^{-1} for all the compositions. The absorption bands observed within these specific limits reveal the formation of single-phase spinel structure having two sub-lattices tetrahedral (A) site and octahedral (B) site **[23]**.

The high frequency band (ν_1) lies in the range 565 to 620cm^{-1} while the low frequency band (ν_2) is varying in the range 418cm^{-1} to 486cm^{-1}. This difference in the band position is expected because of the difference in Fe^{+3}- O^{-2} distance for the tetrahedral and octahedral compounds. Similar observation was seen in the FTIR spectral analysis for the Ni-Mg ferrite system reported by L. John Berchmans, R. Kalai Selvan, P.N. Selva Kumar **[24]**. Waldron **[25]** and Hafner **[26]** have studied the vibrational spectra of ferrites and attributed the High frequency band (ν_1) at around 600cm^{-1} to the tetrahedral site A and low frequency band (ν_2) at around 400cm^{-1} to the octahedral site B.
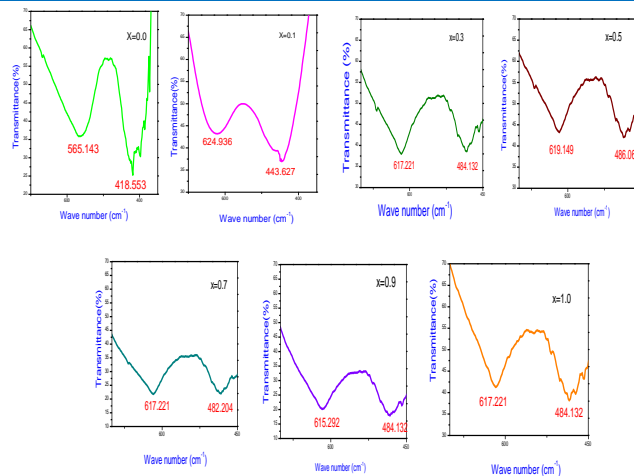

Fig. 8. FTIR patterns of Mg $Cr_xFe_{2-x}O_4$ nano –ferrites with (x=0, 0.1, 0.3, 0.5, 0.7, 0.9, 1)

Table 5. FTIR parameters for Mg-Cr Ferrites.

Ferrite Composition	ν_1 (cm^{-1})	ν_2 (cm^{-1})
$MgFe_2O_4$	565.143	418.553
$MgCr_{0.1}Fe_{1.9}O_4$	624.936	443.627
$MgCr_{0.3}Fe_{1.7}O_4$	617.221	484.132
$MgCr_{0.5}Fe_{1.5}O_4$	619.149	486.161
$MgCr_{0.7}Fe_{1.3}O_4$	617.221	482.204
$MgCr_{0.9}Fe_{1.1}O_4$	615.292	484.132
$MgCrFeO_4$	617.221	484.132

By Cr substitution, broadening of the band around 484 cm^{-1} wave number is observed. The broadening of band is greater at high concentration of Cr. It is found that the positions of the absorption bands are composition dependent which is due to the cation - oxygen bond distances.

Conclusion

- Citrate Gel auto combustion technique is a convenient way for obtaining a homogeneous nano sized mixed Mg-Cr ferrites.
- The process involves no impurity pickup and material loss. It is a very simple and economical method where no specific heating or cooling rate is required. It is a low temperature processing technique and requires shorter sintering duration.
- X-ray diffraction pattern confirms the formation of cubic spinel structure in single phase without any impurity peak. It is in good agreement with the standard data from ICSD
- The crystallite size of the various Mg-Cr ferrites was in the range of 7-23nm.
- The lattice parameter is decreased with the increase of Cr substitution in Mg-Cr ferrites which indicates that the mixed Mg-Cr ferrite system obeys Vegard's law.
- SEM micrographs of various compositions indicate the morphology of the particles is similar. They reveal

largely agglomerated, well defined nano particles of the sample powder with inhomogeneous broader grain size distribution.

- EDS data gives the elemental% and atomic % in the mixed Mg-Cr ferrites and it shows the presence of Mg, Cr, Fe and O without precipitating cations.
- FTIR absorption spectra of the compositions under investigations reveal the formation of a single phase cubic spinel, showing two significant absorption bands.

Reference

1. Surender Kumar, Tukaram J. Shinde, Pramod N. Vasambekar. *Adv. Mat. Lett.* **2013**, *4(5)*, 373.
   DOI: 10.5185/amlett.2012.10429
2. Dixit, Gagan.; Singh, J.P.; Srivastava, R.C.; Agarwal, H.M.; Chaudhary, R.J. *Adv. Mat. Lett.* **2012**, *3(1)*, 21.
   DOI: 10.5185/amlett.2011.6280
3. T. Giannakopoulou; L. Kompotiatis; A. Kontogeorgakos; G. Kordas. *J. Magn. Magn. Mater.* **2002**, *246*, 360.
   DOI: 10.1016/S0304-8853(02)00106-3
4. M.A. Ahmed, *Phy. Status solidi A.* **1989**, *111*, 567.
   DOI: 10.1002/pssa.2211110222
5. E. Olsen; J. Thonstad, *J. Appl. Electrochem.* **1999**, *29*, 293.
   DOI: 10.1023/A:1003464304488
6. Kaur, Balwinder.; Arora, Manju.; Shankar, Ajay.; Srivastava, Avanish Kumar.; Pant, Rajendra Prasad. *Adv. Matt. Lett.* **2012**, *3(5)*, 399.
   DOI: 10.5185/amlett.2012.7288
7. E.W. Gorter, *Nature.* **1950**, *165*, 798.
   DOI: 10.1038/165798a0
8. G. Blasse, *Philips Res.Rep.Supple.* **1964**, *3*, 91.
9. A.K.M. Zakaria; M.A. Abgar; S.G. Eriksson; F.U. Ahmed; S.M. Yunus; H. Rundlof, *J. Magn. Magn. Mater.* **2003**, *265*, 311.
   DOI: 10.1016/S0304-8853(03)00280-4
10. A.K.M. Zakaria; M.A. Abgar; S.G. Eriksson; F.U. Ahmed; S.M. Yunus; R. Delaplane; V. Stanliu; P. Svedlindle, *Mater. Res. Bull.* **2004**, *39*, 1141.
    DOI: 10.1016/j.materresbull.2004.02.015
11. L.B. Kong; Z.W,Li; G.Q. Lin; Y.B. Gan, *J.Am.Ceram. Soc.* **2007**, *90*, 2104.
    DOI: 10.1111/j.1551-2916.2007.01691.x
12. Y. Konseoglu; H. Kavas; B. Aktas, *Phys Status Solidi A.* **2006**, *203*, 1595.
    DOI: 10.1002/pssa.200563104
13. V.B. Kawade; G.K. Bichile; K.M. Jadhav; *Mater.Lett.* **2000**, *42*, 33.
    DOI: 10.1016/S0167-577X(99)00155-X
14. Faizuna Nesa; A.K.M. Zakaria; M. A. Saeed khan; S.M. Yunus; A.K, Das; S.G. Eriksson; M.N.J. Khan; D.K. saha; M.A. Hakim, *World J. Condens. Matter Phy.* **2012**, *2*, 27.
    DOI: 10.4236/wjcmp.2012.21005
15. Muhammed Javed Iqbal; Zahoor Ahmad; Turqut Meydan; Yevgen Melikhov, *J. Appl. Phy.* **2012**, *111*, 033906.
    DOI: 10.1063/1.4704197
16. N.M. Patil; S.D. Jadhav; U.B. Sankpal; M.R. Kadam; B.K. Chougule; N.S. Gajbhiye, *Mater. Chem. and Phy.* **2009**, *113*, 233.
    DOI: 10.1016/j.matchemphys.2008.07.066
17. K. Rama Krishna; D. Ravinder; K. Vijaya Kumar; Ch. Abraham Lincon, *World J. condens. Matter Phy.* **2012**, *2*, 153.
    DOI: 10.4236/wjcmp.2012.23025
18. Cullity B.D., *Elements of XRD, Addison Wesley publishing Company, Inc., Reading, Machusetts,* **1959**, *1*, 132.
19. M. J. Iqbal; M. N. Ashiq; P. Hernandez-Gomezb; J. M. Munoz, *J. Magn. Magn. Mater.* **2008**, *320*, 881.
    DOI: 10.1016/j.jmmm.2007.09.005
20. R.C. kumbale; P.A. sheikh; S.S. Kamble; Y.D. kolekar, *J. Alloys Comp.* **2009**, *478*, 599.
    DOI: 10.1016/j.jallcom.2005.03.007
21. B. Viswanathan; V.R.K. Murthy; *Ferrite Materials: Science and Technology, Narosa Publishing House,* **1990**, 4.
22. Suryawanshi. S.S; Deshpand. V; Sawantn. S.R, *J. Mater. Chem. Phy* .**1999**, *59*, 199.
    DOI: 10.1016/S0254-0584(99)00046-2
23. R.M. Mohamed, M.M. Rashad, F.A. Haraz, W. Sigmund, Journal of Magnetism and Magnetic Materials, **2010**, *322,*2058
    DOI: 10.1016/j.jmmm.2010.01.034
24. L. John Berchmans; R. Kalai Selvan; P.N. Selva Kumar; C.O. Augustin, *J. Magn. Magn. Mater.* **2004**, *279*, 103.
    DOI: 10.1016/j.jmmm.2004.01.073
25. R.D. Waldron, *Phys. Rev.* **1955**, *99*, 1727.
    DOI: 10.1103/PhysRev.99.1727
26. Sr. Hafner, *Zeitschrift für Kristallographie - Crystalline Materials.* **1961**, *115*, 331.
    DOI: 10.1524/zkri.1961.115.5-6.331